FERMILAB Proposal No.: 588

Scientific Spokesman:

John Elias
Fermilab
840-4135

INCLUSIVE POWER LAW DISTRIBUTIONS FOR NON-LEADING PARTICLES PRODUCED IN HADRON COLLISIONS

A. E. Brenner, D. C. Carey, J. E. Elias, P. H. Garbincius and V. A. Polychronakos
Fermi National Accelerator Laboratory, Batavia, Illinois 60510

and

D. Cutts, R. Dulude, R. E. Lanou, and J. T. Massimo
Brown University, Providence, Rhode Island 02912

and

M. T. Chiaradia, C. DeMarzo, C. Favuzzi, G. Germinario, L. Guerriero, P. LaVopa, G. Maggi, F. Posa, G. Selvaggi, P. Spinelli and F. Waldner
Istituto di Fisica and INFN, Bari, Italy

January 27, 1978

INCLUSIVE POWER LAW DISTRIBUTIONS FOR NON-LEADING PARTICLES PRODUCED IN HADRON COLLISIONS

A. Brenner, D. Carey, J. Elias, P. Garbincius, V. Polychronakos (Fermilab); D. Cutts, R. Dulude, R. Lanou, J. Massimo (Brown University); M. Chiaradia, C. DeMarzo, C. Favuzzi, G. Germinario, L. Guerriero, P. LaVopa, G. Maggi, F. Posa, G. Selvaggi, P. Spinelli, F. Waldner (Istituto di Fisica and INFN)

A study of single particle inclusive spectra using the Single Arm Spectrometer (SAS) in the M6E beam line is proposed. The principal objective is a determination of the power law behavior, $(1-x)^n$, of non-leading reactions in the beam fragmentation region. This experiment which extends the measurements made earlier in E-118A will span a kinematic range of $.3 \leq x \leq .88$ mostly at $p_T=0.3$ and 0.5 at an incident momentum of 100 GeV/c. Particular emphasis will be placed on reactions initiated by kaons and $\bar{p}$'s. Most of the minority channels will be measured to the 10-20% level.

Recent work, both experimental and theoretical, has indicated that hadron-hadron inclusive reactions at small as well as large p_T provide considerable insight into the understanding of the internal structure of the hadrons. Kaon initiated reactions will provide information on the valence s and $\bar{s}$ distributions in the kaon, and similarly, the inclusive kaon spectra would probe s and $\bar{s}$ distributions in the hadron sea.

This experiment uses the apparatus of E-118A, with the deletion of the target area multiplicity detector. This allows for an incident flux of 5-10 times that which was possible in the earlier experiment. The π^0 detector built for E-451 (also an SAS experiment) will be the only added piece of equipment.

The π^0 detector will be used to implement a second independent trigger to simultaneously study inclusive π^0 spectra in the range $0 < x_R < 0.8$ and with p_T up to ~ 4.0. This measurement will improve existing data by about an order of magnitude in sensitivity and will explore a new kinematic region.

With a flux of 10^7 particles onto the hydrogen target per accelerator pulse, the measurements will require 500 hours of average quality beam time. An additional 100 hours will be required for start-up and spectrometer tuning.

January, 1978

I. INTRODUCTION

The picture of the nucleons as composite systems consisting of partons[1] emerged with the discovery of scaling in deep inelastic electron-proton scattering[2]. The idea that partons are quarks proved to be particularly useful for the study of lepton-hadron couplings. This concept and the success of the naive quark model in describing the hadron multiplets suggest naturally an underlying link at the quark level between hadron and lepton-induced multiparticle production phenomena. Experimentally one observes a striking similarity in the logarithmic rise of the mean charged particle multiplicity with energy in both processes. Furthermore, the limited transverse momentum structure of the hadronic jets in electron-positron annihilations with respect to the jet axis resembles the limited transverse momentum distributions common with particles produced in purely hadronic interactions. In spite of these similarities the approaches that have been used to describe these phenomena have little in common. Distributions for purely hadronic interactions are usually understood in the framework of Regge theory, diffractive scattering, thermodynamic models, etc., whereas for the lepton induced phenomena one invokes local currents, quark-parton models, etc.

The ideas of the quark-parton models have been applied, until recently, only in the hadronic production of particles with high transverse momentum since such phenomena are believed to be the result of short range interactions probing the internal structure of hadrons. Recently, experimental evidence has prompted attempts to extend the quark-parton ideas to include low p_T phenomena. In particular, a relationship has been observed between the longitudinal spectra of pions produced in proton-proton interactions at high energies and the quark structure functions as measured in lepton-proton interactions. Therefore, low p_T phenomena are proving to be important in understanding the internal structure of hadrons, especially the dynamics of multiparticle production from elementary constituent interactions.

We propose to extend our investigation of single particle inclusive spectra in the projectile fragmentation region by an intensive concentration on those rarer channels which could not be adequately covered in our recently completed survey experiment, E118A. In particular, we wish to concentrate on kaon and $\bar{p}$ driven reactions, plus a few other rare processes. A modest alteration in our apparatus will allow an order of magnitude greater sensitivity to these reactions. Our E118A results have allowed rough estimates of the rates of these reactions, and have guided our proposal for further investigation. Combined with our results from E118A, these new data will provide measurements of inclusive cross sections for a wide variety of incident and produced particle types. This will be essential in unraveling the influence of constituent type on the dynamics of multiparticle production. Thus, we can possibly establish the link between the short-range high transverse momentum phenomena and the relatively long-range low p_T interactions.

II. PHYSICS BACKGROUND

The preliminary analysis of experiment E118A and other FNAL and ISR experiments support the idea that there exists an underlying connection between low p_T phenomena and quark-parton ideas. The ISR data first showed that the inclusive pion spectra in pp interactions exhibit a power law behaviour similar to the observed $\nu W_2(x)$ at SLAC, i.e., $d\sigma/dx(pp \rightarrow \pi^+X) \sim (1 - x)^3$. This led Ochs[3] to speculate that these pions are fragments of the quarks in the proton. Brodsky and Gunion[4] then cite Och[3] in predicting that at large x[4]

$$R(\pi^+/\pi^-) = \frac{d\sigma/dx(pp \rightarrow \pi^+X)}{d\sigma/dx(pp \rightarrow \pi^-X} = \frac{Gu/p(x)}{Gd/p(x)}$$

where $G_{u/p}(x)$ and $G_{d/p}(x)$ are the u and d quark distributions in a proton respectively. It then follows that

$$\frac{\nu W_2^{en}}{\nu W_2^{ep}} = \frac{4+R}{4R+1}$$

This relation is well satisfied over the range $0<x<1$ as shown in Figure 1, which is reproduced from Reference 3. Furthermore, the ratio R appears to be approaching 5 at $x \simeq 1$ or equivalently $\nu W_2^{en}/\nu W_2^{ep} \rightarrow 3/7$ a value predicted by Farrer and Jackson[5] in a quark-vector gluon model if the helicities of the proton and the leading quark are the same for $x \rightarrow 1$. In addition, R appears to be independent of p_T. In Figure 2, R, as calculated from our E118A data, is plotted against x along with the values from

Antreasyan *et. al.*,[6] from a high p_T experiment plotted against $x_\perp$. It appears that R has the same behaviour as $x \to 1$ in the beam direction and as $x_\perp \to 1$ at 90^o. The same appears to be true with the K^+/K^- ratio as shown in Figure 3.*

Yet another aspect of the power law behaviour of the inclusive spectra seems to favour the quark-parton model. In Figures 4 and 5 the x-distributions are plotted for various particle species in π^+ and p induced reactions respectively at $p_T = 0.3$ GeV/c and incident momentum of 100 GeV/c. The solid lines in these figures represent fits of the data to the form $A(1-x)^{n_h}$. The values of the exponent n_h are tabulated in Table I for the various hadrons. In the same table the exponents from fits to the data at $p_T = 0.5$ and 0.75 GeV/c are shown. They appear to be nearly independent of p_T at least in the p_T region between 0.3 and 0.8 GeV/c. This constant power law behaviour is characteristic of most constituent models[7,8], in contrast to predictions from multi-Regge expansions in which the distributions behave as $d\sigma/dxdt \sim \beta(t)(1-x)^{1-2\alpha(t)}$ where $\alpha(t)$ is the leading trajectory and the power should approach zero at small $t \sim p_T^2$.

As the quark-parton models become more quantitative one expects that the longitudinal inclusive spectra will be of great importance in understanding the constituent picture of hadrons. In particular, we will look at mesons, which cannot be studied in lepton-induced reactions. The "unfavoured" reactions

---

*Similar behaviour was observed by J. R. Johnson *et. al.*[10] who plot their data as a function of $x_R = E^*/E_{max}$.

e.g., $\pi^+ p \to K^- X$, $pp \to K^- X$ which we intend to emphasize in this experiment should be particularly useful since they are free from leading particle and other effects which make the interpretation of "favoured" processes more difficult. Kaon spectra for example, probe the s and $\bar{s}$ distributions in the hadron sea, whereas kaon induced reactions provide information on the valence s and $\bar{s}$ distributions in these mesons. An attempt to this direction has already been made by Duke and Taylor[9] who used data from a FNAL experiment[10] to determine the sea distributions in the proton with some interesting results as to the fraction of momentum carried by the sea quarks.

III. THE PROPOSED EXPERIMENT

We propose to pursue further the exploration of single particle inclusive reactions started with E118A using the Single Arm Spectrometer (SAS) and the M6E beam line. The spectrometer has been successfully operating for several years and has been described elsewhere[11]. Briefly we can measure and identify hadrons produced with momentum between P_{max} and 20 GeV/c and at angles between 3 and 19 mr in the laboratory system. The corresponding Feynman-x range extends from x = 0.2 to x = 0.95 for 100 GeV/c incident momentum. The range for p_T is from $p_T \simeq 0$ to $p_T \simeq 1.2$ GeV/c.

This experiment differs from E118A in that we do not plan to use the associated charged multiplicity detector used in E118A. This will enable us to increase the incident flux by a factor of 5 to 10 improving the statistical accuracy for the "minority" or "unfavoured" channels. Prescaling of the dominant incident particles will allow further emphasis of the minority channels. In addition, the target empty background rate will be reduced to about 4% of the target full rate.

Another major difference is the use in this experiment of the π^0 detector being installed for experiment E451. This detector will be used as a second independent trigger to study inclusive π^0 spectra over the wide kinematic range shown in Figure 6. The detector is centered at 90 mrad in the LAB (65 degrees in the CM), allowing simultaneous coverage of both the central $x \simeq 0$ region and the fragmentation region out to the kinematic limit at $p_T = 3.0$ GeV/c. The π^0 detector subtends 15 mster in the Laboratory and will determine the p_T of the π^0 to about 10% by measuring the shower position and energy. This will allow, for the first time, an extensive coverage in x and p_T for inclusive π^0 production by both proton and meson beams.

Two other groups working at Fermilab have studied π^0 production. E63 studied radial scaling[12] in pp interactions and E268 compared the production of π^0 by proton and pion beams[13] at essentially 90° in the center of mass. We propose to study the ratio

$$E \frac{d^3\sigma}{dp^3} (\pi^+ p \to \pi^0 X) \Big/ E\frac{d^3\sigma}{dp^3}(pp \to \pi^0 X)$$

as a function of both x and p_T, extending coverage in the radial x variable to $x_R \approx 0.8$ and a major improvement in statistics at lower x_R.

Our preliminary plans are to restrict ourselves to an incident momentum of 100 GeV/c only and to accumulate data at $p_T = 0.3$, and $p_T = 0.5$ GeV/c for all 4 combinations of charge sign in the beam and the spectrometer. The x-range to be covered will extend from x = 0.3 to x = 0.88. In addition, data will be taken at $p_T = 0.75$ for one x-value only, x = 0.3, to complement existing data from E118A and provide a p_T dependence of the cross sections from $p_T \sim .15$ GeV/c to $p_T = .75$ GeV/c.

IV. RATES AND RUNNING TIME

The expected counting rates per one hour running time for all possible channels are shown in Table II. All the rates were calculated at x = 0.3 and $p_T = 0.3$ GeV/c and are based on the following conditions.

1) The cross sections were taken from the preliminary E118A results. To calculate rates at kinematic points where no data were available the measured p_T and x dependence for the appropriate channels were used to extrapolate the measured cross sections to these points.
2) The spectrometer tune used is the same as in E118A. It provides an effective phase space acceptance of 32 μster%.
3) The same 20" liquid hydrogen target as in E118A was used.

4) An incident flux of 10^7 particles per accelerator pulse was used with the particle composition shown in Table III. Experiment E99 recently ran at the facility at comparable rates experienced no problems with the beam tagging system other than a slight increase of double buckets. Finally, we estimated a pulse repetition rate of 5 pulses/minute.

The total running time required to accumulate enough events for a 10 to 20% statistical accuracy for most minority channels, at $p_T = 0.3$ and 0.5 GeV/c, is estimated to be approximately 500 hours. It has been our experience that an additional 50 to 100 hours is required for start-up and spectrometer tune. In Table IV are shown the time estimates for 10% statistics for the indicated minority channel as well as estimated yields for certain other minority channels for positive beam. Table V shows the same for negative beam. Finally in Table VII are shown the yields for selected channels for a 12 hour run at $p_T = 0.75$ GeV/c.

The same luminosity considerations were used to calculate the expected rates in the π^0 detector. We again emphasize that only one setting is required to cover the kinematic range outlined in Figure 1. The proton induced rate was based on an extrapolation of the radial scaling parametrization.(12) The pion/proton beam rations at all x were assumed to be those measured at 90^0 in the center of mass.(13) Table VI lists the data rate per hour in a bin $\Delta p_T = 1.0$ GeV GeV/c, and $\Delta x = 0.10$ centered for $p_T = 3.0$ GeV/c for various x values. This shows that we can obtain a 10%

measurement of the cross sections at $p_T = 3.0$ GeV/c out to

$$x = 0.45 \quad \text{for} \quad pp \to \pi^0 X$$

$$x = 0.55 \quad \text{for} \quad \pi^+ p \to \pi^0 X$$

$$x = 0.62 \quad \text{for} \quad \pi^- p \to \pi^0 X$$

REFERENCES

1. R. P. Feynman, Photon-Hadron Interactions (W. A. Benjamin, New York, 1972); Phys. Rev. Letters 23, 1415(1969).
2. For a review see J. I. Friedman and H. W. Kendall, Rev. Nucl. Sci. 22, 203(1972).
3. W. Ochs, Nucl. Phys. B118, 397(1977).
4. S. J. Brodsky and J. F. Gunion, SLAC-PUB-1820(1976).
5. G. R. Farrar and D. R. Jackson, Phys. Rev. Letters 35,1416(1975).
6. D. Antreasyan et al., Phys. Rev. Letters 38, 112(1977).
7. R. Blankenbecler and S. Brodsky, Phys. Rev. D10, 2973(1974).
8. H. Goldberg, Nucl. Phys. B44, 149(1972).
9. D. W. Duke and F. E. Taylor, FERMILAB-Pub-77/95(1977).
10. J. R. Johnson et al., FERMILAB-Pub-77/98(1977), and FERMILAB-Pub-77/99(1977).
11. J. Butler, Ph.D. Thesis, unpublished, MIT(1975); D. S. Ayres et al., Phys. Rev. D15, 3105(1977).
12. D. C. Carey et al., Phys. Rev. D14,1196(1976).
13. G. Donaldson et al., Phys. Rev. Letters 36,1110(1976).

TABLE CAPTIONS

TABLE I Exponents of the power law fits to the E118A data.

TABLE II Event rate/hr for 10^7 incident particles/pulse and and 5 pulses/min at x=0.3.

TABLE III Composition of the M6E beam line for 400 GeV/c primary protons.

TABLE IV Run plan and estimated yields for selected channels initiated by positive beam.

TABLE V Run plan and estimated yields for selected channels initiated by negative beam.

TABLE VI π^0 event rate/hr for 10^7 incident particles/pulse and 5 pulses/min at 100 GeV/c incident momentum and at x=0.3.

TABLE VII Estimated yields for selected channels for 6 hours running time at p_T=0.75 GeV/c and x=0.3.

FIGURE CAPTIONS

Fig. 1: Comparison of the neutron-proton ratio in deep inelastic scattering, and inclusive $\pi^{\pm}$ production in pp interactions (Ref. 3 and references therein).

Fig. 2: Ratios of the invariant cross sections for π^+, and π^- production from experiment E118A, and from an experiment at 90^o in the CM (Ref. 6).

Fig. 3: Ratios of the invariant cross sections for K^+, and K^- production from experiment E118A, and from an experiment at 90^o in the CM (Ref. 6).

Fig. 4: Invariant cross sections for the production of $\pi^+(\times)$, $\pi^-(\bullet)$, $K^+(\blacktriangle)$, $K^-(\blacktriangledown)$, $p(\blacksquare)$, $\bar{p}(\blacklozenge)$ in π^+p interactions as functions of Feynman-x at 100 GeV/c incident momentum, and at p_T=0.3 GeV/c (from E118A).

Fig. 5: Invariant cross sections for the production of $\pi^+(\bullet)$, $\pi^-(\blacklozenge)$, $K^+(\blacktriangle)$, $K^-(\blacktriangledown)$, $p(+)$, $\bar{p}(\blacksquare)$ in pp interactions as functions of Feynman-x at 100 GeV/c incident momentum, and at p_T=0.3 GeV/c(from E118A).

Fig. 6: Acceptance of the π^o detector positioned as described in the text, and at incident momentum of 100 GeV/c.

TABLE I

EXPONENTS OF THE POWER LAW FITS TO THE E118A DATA

	$\pi^+p\to hX$				$\bar{p}p\to hX$		
h \ p_T		n_h	Average n_h	h	p_T	n_h	Average n_h
K^+	0.3	0.56±0.11		K^+	0.3	2.89±0.12	
	0.5	0.68±0.07	0.73±0.05		0.5	2.93±0.09	2.94±0.06
	0.75	0.97±0.10			0.75	3.01±0.12	
p	0.3	1.53±0.13		K^+	0.3	1.60±0.22	
	0.5	1.30±0.09	1.39±0.06		0.5	2.01±0.12	1.95±0.09
	0.75	1.42±0.11			0.75	2.06±0.19	
π^-	0.3	1.10±0.10		π^-	0.3	3.66±0.14	
	0.5	1.99±0.18	1.47±0.07		0.4	4.20±0.12	3.92±0.08
	0.75	1.82±0.13			0.5	3.78±0.16	
K^-	0.3	1.83±0.14		K^-	0.3	4.45±0.28	4.42±0.24
	0.5	2.43±0.32	1.89±0.11		0.5	4.33±0.46	
	0.75	1.80±0.20					
$\bar{p}$	0.3	2.42±0.18	2.43±0.16	$\bar{p}$	0.3	6.06±0.47	6.65±0.13
	0.5	2.46±0.32			0.5	6.69±0.13	

TABLE II

EVENT RATE/HR FOR 10^7 INCIDENT PARTICLES/ PULSE AND 5 PULSES/MIN

x=0.3

In	Out	π^+	K^+	p	π^-	K^-	$\bar{p}$
100 GeV/c			p_T=0.3 GeV/c				
π^+		3491	371	299	1903	262	137
K^+		146	103	11	117	17	12
p		2012	181	1808	939	64	20
π^-		2697	334	356	5410	451	304
K^-		103	21	10	178	125	11
$\bar{p}$		106	31	11	180	7	123
100 GeV/c			p_T=0.5 GeV/c				
π^+		1298	213	210	930	91	65
K^+		91	65	10	42	5	5
p		862	141	923	432	22	15
π^-		1519	147	182	2795	272	176
K^-		32	26	13	74	42	9
$\bar{p}$		62	15	5	65	4	77

TABLE III

COMPOSITION OF THE M6E BEAM LINE FOR 400 GeV/c PRIMARY PROTONS

Secondary momentum	p	π^+	K^+	$\bar{p}$	π^-	K^-
100 GeV/c	0.380	0.570	0.039	0.034	0.920	0.047
150 GeV/c	0.630	0.330	0.032	0.022	0.940	0.049
175 GeV/c	0.720	0.230	0.030	0.015	0.950	0.044

TABLE IV

RUNPLAN AND ESTIMATED YIELDS FOR SELECTED CHANNELS INITIATED BY POSITIVE BEAM

1. +BEAM +SAS

p_T = 0.3 GeV/c

x	(hrs) Time	(events) $K^+\to p$	$K^+\to p^+$	$K^+\to K^+$
0.3	4.0	50	580	400
0.4	4.0	50	1100	960
0.5	4.0	50	1400	1140
0.6	5.0	50	2670	1400
0.7	5.0	50	580	1600
0.8	5.0	50	860	3750
0.88	5.0	35	430	5700

p_T = 0.5 GeV/c

x	(hrs) Time	(events) $K^+\to\pi^+$	$p\to K^+$	$K^+\to K^+$	$K^+\to p$
0.3	1.5	300	600	200	45
0.4	1.5	300	600	270	35
0.5	2.0	300	400	600	20
0.6	2.0	300	400	650	20
0.7	2.5	300	500	900	15
0.8	2.5	300	250	2400	3
0.88	3.0	300	300	3000	

2. +BEAM → -SAS

p_T = 0.3 GeV/c

x	(hrs) Time	(events) $K^+\to\pi^-$	$\pi\to\bar{p}$	$K^+\to K^-$	$K^+\to\bar{p}$	$p\to K^-$	$p\to\bar{p}$
0.3	2.5	300	250	30	20	160	35
0.4	2.5	300	250	20	15	200	20
0.5	3.0	300	300	30	6	150	6
0.6	3.5	300	350	20		50	
0.7	3.5	300	250			20	
0.8	4.0	300	80				
0.88	4.0	200	70				

p_T = 0.5 GeV/c

x	(hrs) Time	(events) $K^+\to\pi^-$	$K^+\to K^-$	$K^+\to\bar{p}$	$p\to K^-$	$p\to\bar{p}$
0.3	2.5	100	14	30	55	37
0.4	2.5	100	13	25	45	20
0.5	2.5	100	12	25	40	9
0.6	2.5	100	5	10	20	
0.7	3.0	100		4		
0.8	3.0	100				
0.88	3.0	100				

TABLE V

RUN PLAN AND ESTIMATED YIELDS FOR SELECTED CHANNELS INITIATED BY NEGATIVE BEAM

1. -BEAM → -SAS

	$p_T = 0.3$ GeV/c						$p_T = 0.5$ GeV/c					
	(hrs)	(events)					(hrs)	(events)				
x	Time	$\bar{p}\to\pi^-$	$\bar{p}\to K^-$	$K^-\to\pi^-$	$K^-\to K^-$	$K^-\to\bar{p}$	Time	$\bar{p}\to\pi^-$	$\bar{p}\to K^-$	$K^-\to\pi^-$	$K^-\to K^-$	$K^-\to\bar{p}$
0.3	1.0	100	7	160	120	25	1.0	100	40	100	150	15
0.4	1.0	100	20	200	190	25	1.5	100	50	130	230	20
0.5	1.0	100	25	230	230	20	2.0	100	35	220	310	15
0.6	2.0	100	30	400	700	20	2.5	100	20	185	475	15
0.7	3.0	100	70	600	1500		3.0	100	10	350	390	8
0.8	4.0	100	100	700	3200		3.0	100		230	680	
0.88	6.0	100	160	700	7400		3.0	100		150	875	

2. -BEAM → +SAS

	$p_T = 0.3$ GeV/c						$p_T = 0.5$ GeV/c						
	(hrs)	(events)					(hrs)	(events)					
x	Time	$K^-\to\pi^+$	$K^-\to K^+$	$K^-\to p$	$\bar{p}\to\pi^+$	$\bar{p}\to p$	Time	$K^-\to\pi^+$	$K^-\to K^+$	$K^-\to p$	$\bar{p}\to\pi^+$	$K^-\to\bar{p}$	$\bar{p}\to p$
0.3	2.0	200	40	20	200	20	2.0	200	50	30	120	22	18
0.4	2.0	200	36	20	160	8	2.0	200	40	30	100	44	6
0.5	2.0	200	36	18	180		2.0	100	25	26	60	30	
0.6	2.0	200	28	10	100		3.0	100	12	25	45	18	
0.7	2.0	200	8		80		3.0	100	25	15	40	18	
0.8	3.0	150			45		4.0	100			18	15	
0.88	4.0	100			17		4.0	100			6	10	

TABLE VI

π^0 EVENT RATE/HR FOR 10^7 INCIDENT PARTICLES PER PULSE AND 5 PULSES/MIN

	100 GeV/c	p_T=3.0 GeV/c	
x	$pp\to\pi^0X$	$\pi^+p\to\pi^0X$	$\pi^-p\to\pi^0X$
0.0	5.7	16.5	27.3
0.1	5.2	15.3	24.9
0.2	4.1	11.9	19.6
0.3	2.8	8.0	13.4
0.4	1.6	4.5	7.7
0.5	0.72	2.1	3.4
0.6	0.25	0.72	1.2
0.7	0.05	0.15	0.24
0.8	0.01	0.02	0.05

TABLE VII

ESTIMATED YIELDS FOR SELECTED CHANNELS FOR 6 HRS RUNNING AT p_T=0.75 GeV/c and x=0.3

	Evts/6 hrs		Evts/6 hrs
$K^+ \to \pi^+$	100	$K^+\to \pi^-$	90
$K^+ \to K^+$	120	$K^+\to K^-$	90
$K^+ \to p$	35	$K^+\to \bar{p}$	15
$p \to K^+$	150	$p \to K^-$	146
		$p \to \bar{p}$	50

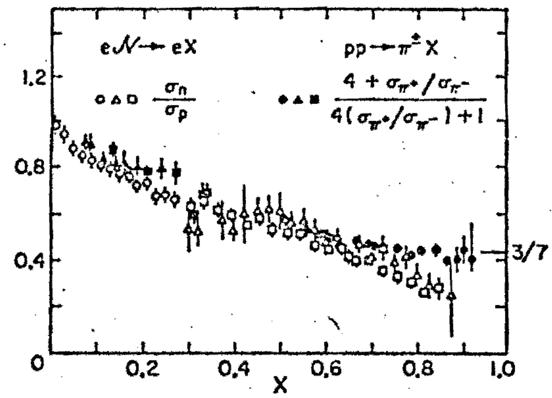
eN → eX
pp → π± X
○△□ σn/σp
●▲■ (4 + σπ+/σπ−)/(4(σπ+/σπ−) + 1)
1.2
0.8
0.4
0
0.2
0.4
0.6
0.8
1.0
X
3/7

Fig. 1

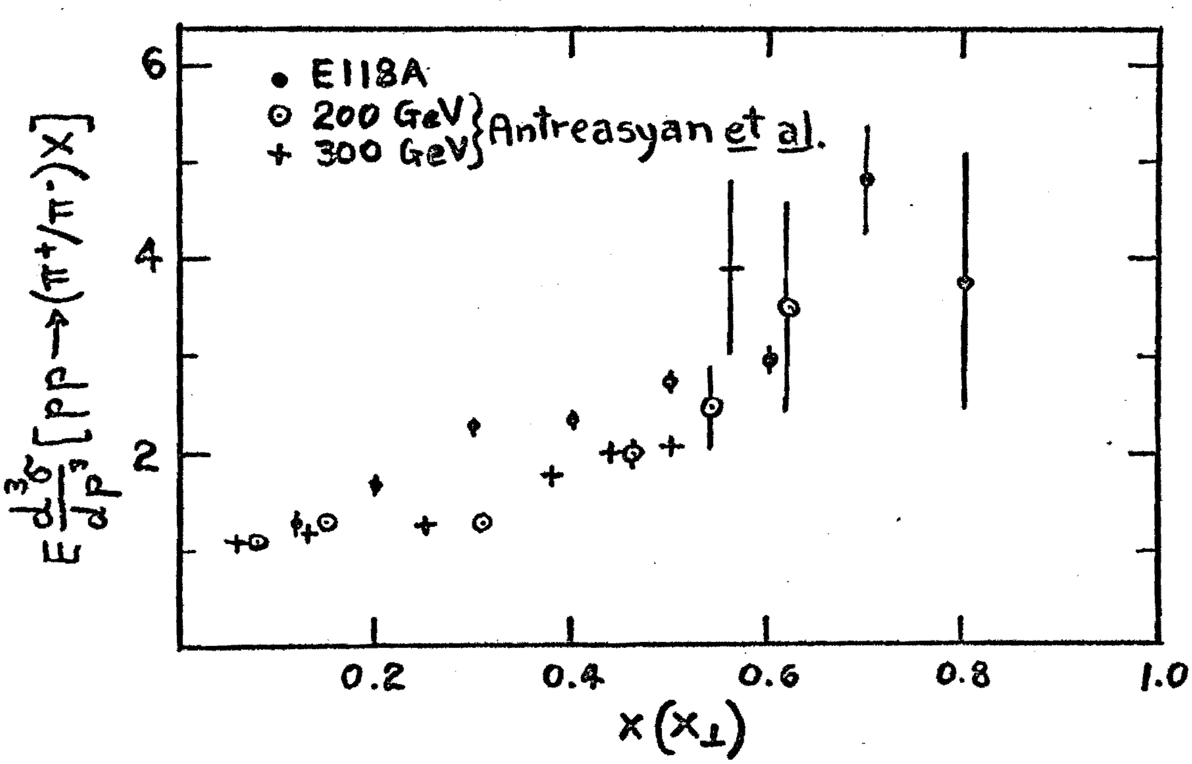
● E118A
⊙ 200 GeV
+ 300 GeV
Antreasyan et al.
E d³σ/dp³ [pp → (π⁺/π⁻)X]
6
4
2
0.2
0.4
0.6
0.8
1.0
x (x⊥)

Fig. 2

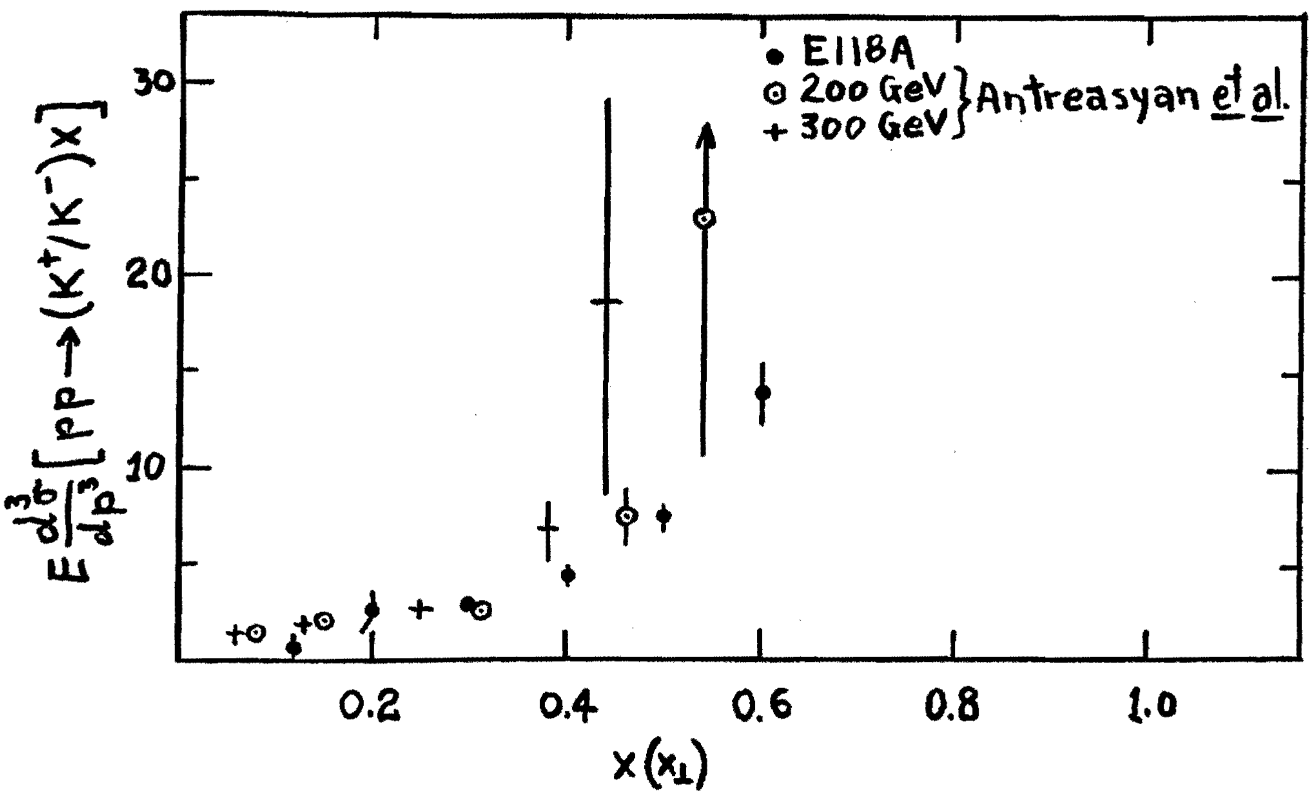

• E118A
⊙ 200 GeV
+ 300 GeV
Antreasyan et al.
30
20
10
0.2
0.4
0.6
0.8
1.0
X (x⊥)
E d³σ/dp³ [pp → (K⁺/K⁻) X]

Fig. 3

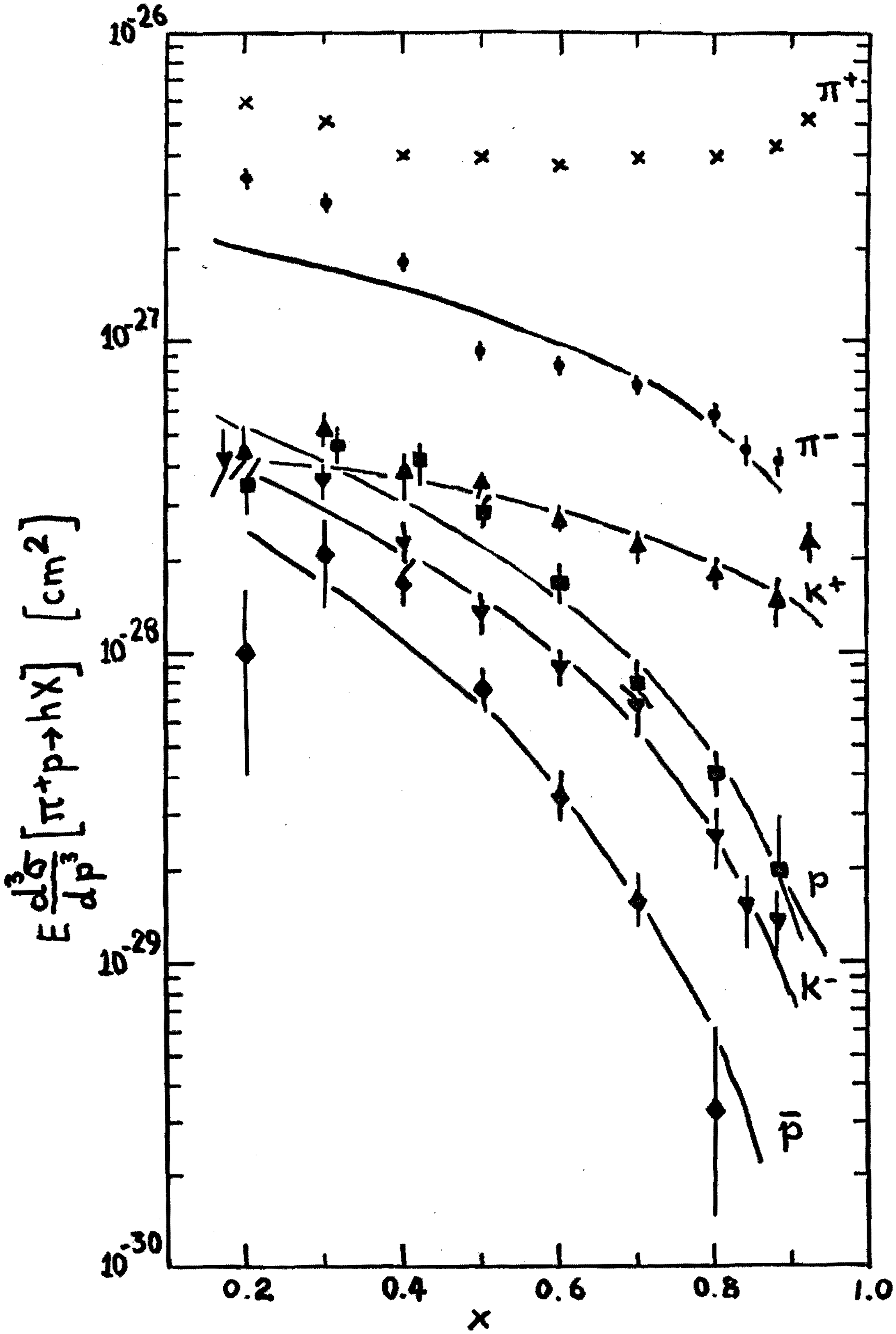
10^{-26}
10^{-27}
10^{-28}
10^{-29}
10^{-30}
π^+
π^-
K^+
p
K^-
$\bar{p}$
$E\frac{d^3\sigma}{dp^3}[\pi^+p\to hX]$ [cm^2]
0.2
0.4
0.6
0.8
1.0
X

Fig. 4

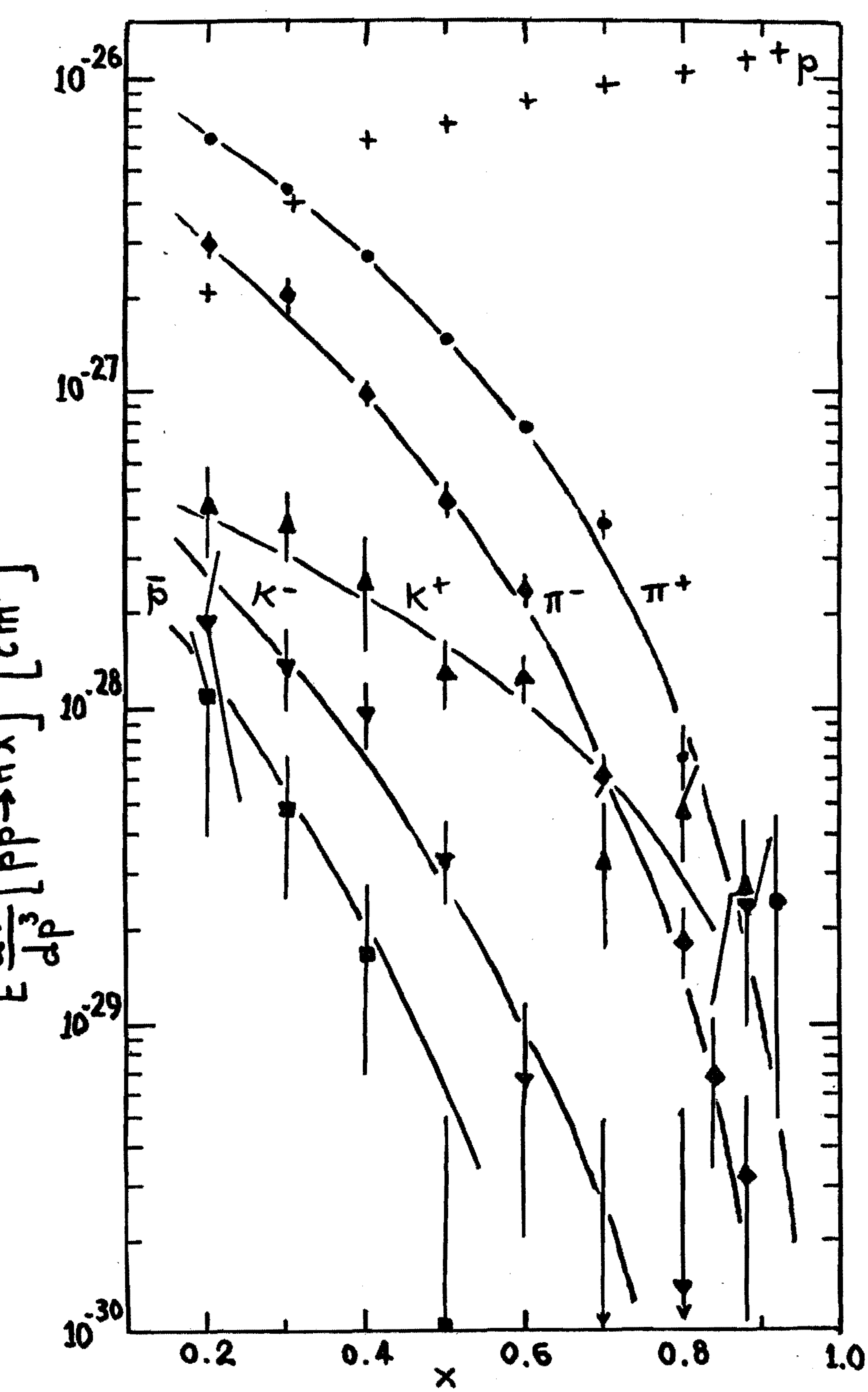

10^{-26}
10^{-27}
10^{-28}
10^{-29}
10^{-30}
$E\frac{d^3\sigma}{dp^3}[pp \to hX]$ [cm^2]
0.2
0.4
0.6
0.8
1.0
x
p
$\bar{p}$
K^-
K^+
π^-
π^+

Fig. 5

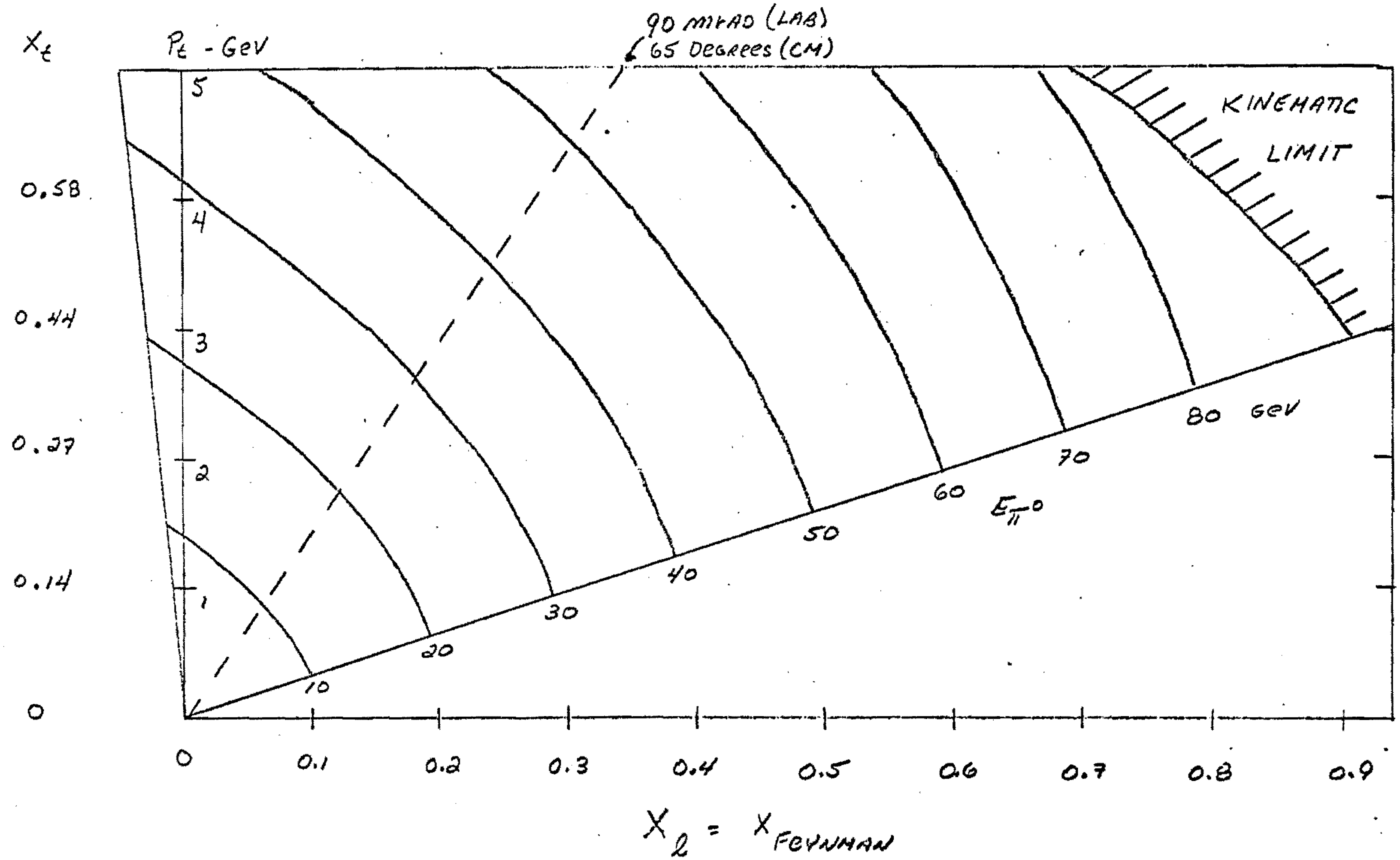

Figure 6: 100 GEV π^0 Production Kinematic Range Accepted by Lead Glass Detector